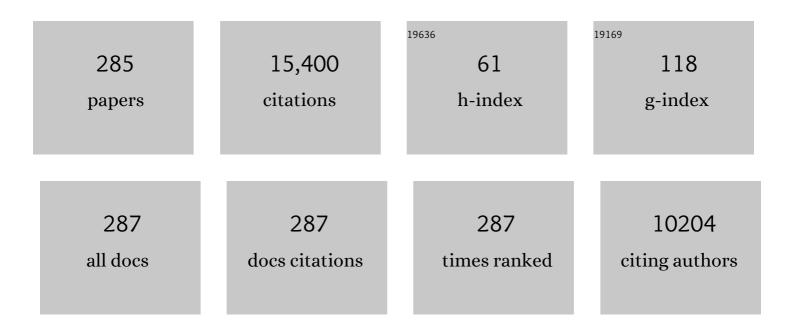
List of Publications by Year in descending order

Source: https://exaly.com/author-pdf/3419948/publications.pdf Version: 2024-02-01



ICAL RDENED

#	Article	IF	CITATIONS
1	Highâ€Efficiency Dielectric Huygens' Surfaces. Advanced Optical Materials, 2015, 3, 813-820.	3.6	1,045
2	Tailoring Directional Scattering through Magnetic and Electric Resonances in Subwavelength Silicon Nanodisks. ACS Nano, 2013, 7, 7824-7832.	7.3	917
3	Enhanced Third-Harmonic Generation in Silicon Nanoparticles Driven by Magnetic Response. Nano Letters, 2014, 14, 6488-6492.	4.5	522
4	Thin-film sensing with planar terahertz metamaterials: sensitivity and limitations. Optics Express, 2008, 16, 1786.	1.7	454
5	Spectrally selective chiral silicon metasurfaces based on infrared Fano resonances. Nature Communications, 2014, 5, 3892.	5.8	397
6	Realizing Optical Magnetism from Dielectric Metamaterials. Physical Review Letters, 2012, 108, 097402.	2.9	381
7	1.5-μm-band wavelength conversion based on cascaded second-order nonlinearity in LiNbO3waveguides. IEEE Photonics Technology Letters, 1999, 11, 653-655.	1.3	352
8	Polarization-Independent Silicon Metadevices for Efficient Optical Wavefront Control. Nano Letters, 2015, 15, 5369-5374.	4.5	344
9	Resonantly Enhanced Second-Harmonic Generation Using III–V Semiconductor All-Dielectric Metasurfaces. Nano Letters, 2016, 16, 5426-5432.	4.5	341
10	Active Tuning of All-Dielectric Metasurfaces. ACS Nano, 2015, 9, 4308-4315.	7.3	340
11	THz near-field imaging. Optics Communications, 1998, 150, 22-26.	1.0	339
12	Ultrafast all-optical tuning of direct-gap semiconductor metasurfaces. Nature Communications, 2017, 8, 17.	5.8	300
13	A spatial light modulator for terahertz beams. Applied Physics Letters, 2009, 94, .	1.5	271
14	Broken Symmetry Dielectric Resonators for High Quality Factor Fano Metasurfaces. ACS Photonics, 2016, 3, 2362-2367.	3.2	271
15	Multiple-channel wavelength conversion by use of engineered quasi-phase-matching structures in LiNbO_3 waveguides. Optics Letters, 1999, 24, 1157.	1.7	247
16	Femtosecond optical polarization switching using a cadmium oxide-based perfect absorber. Nature Photonics, 2017, 11, 390-395.	15.6	245
17	Efficient Polarization-Insensitive Complex Wavefront Control Using Huygens' Metasurfaces Based on Dielectric Resonant Meta-atoms. ACS Photonics, 2016, 3, 514-519.	3.2	229
18	Electrically tunable all-dielectric optical metasurfaces based on liquid crystals. Applied Physics Letters, 2017, 110, .	1.5	221

#	Article	IF	CITATIONS
19	Theory of epsilon-near-zero modes in ultrathin films. Physical Review B, 2015, 91, .	1.1	215
20	Enhanced Second-Harmonic Generation Using Broken Symmetry III–V Semiconductor Fano Metasurfaces. ACS Photonics, 2018, 5, 1685-1690.	3.2	204
21	Optical magnetic mirrors without metals. Optica, 2014, 1, 250.	4.8	188
22	Terahertz emission in single quantum wells after coherent optical excitation of light hole and heavy hole excitons. Physical Review Letters, 1992, 69, 3800-3803.	2.9	178
23	Epsilon-Near-Zero Strong Coupling in Metamaterial-Semiconductor Hybrid Structures. Nano Letters, 2013, 13, 5391-5396.	4.5	178
24	An all-dielectric metasurface as a broadband optical frequency mixer. Nature Communications, 2018, 9, 2507.	5.8	173
25	Observation of Fano Resonances in Allâ€Dielectric Nanoparticle Oligomers. Small, 2014, 10, 1985-1990.	5.2	164
26	Coherent control of terahertz charge oscillations in a coupled quantum well using phase-locked optical pulses. Physical Review B, 1993, 48, 4903-4906.	1.1	162
27	Single-mode GaN nanowire lasers. Optics Express, 2012, 20, 17873.	1.7	146
28	Coherent terahertz radiation detection: Direct comparison between free-space electro-optic sampling and antenna detection. Applied Physics Letters, 1998, 73, 444-446.	1.5	145
29	High-harmonic generation from an epsilon-near-zero material. Nature Physics, 2019, 15, 1022-1026.	6.5	137
30	Light-Emitting Metasurfaces: Simultaneous Control of Spontaneous Emission and Far-Field Radiation. Nano Letters, 2018, 18, 6906-6914.	4.5	126
31	Nonlinear Interference and Tailorable Third-Harmonic Generation from Dielectric Oligomers. ACS Photonics, 2015, 2, 578-582.	3.2	124
32	Design and performance of singular electric field terahertz photoconducting antennas. Applied Physics Letters, 1997, 71, 2076-2078.	1.5	123
33	Shaping Photoluminescence Spectra with Magnetoelectric Resonances in All-Dielectric Nanoparticles. ACS Photonics, 2015, 2, 172-177.	3.2	120
34	Microneedleâ€Based Transdermal Sensor for Onâ€Chip Potentiometric Determination of K ⁺ . Advanced Healthcare Materials, 2014, 3, 876-881.	3.9	116
35	Phased-array sources based on nonlinear metamaterial nanocavities. Nature Communications, 2015, 6, 7667.	5.8	115
36	Terahertz near-field microscopy based on a collection mode detector. Applied Physics Letters, 2000, 77, 3496-3498.	1.5	114

#	Article	lF	CITATIONS
37	High Quality Factor Toroidal Resonances in Dielectric Metasurfaces. ACS Photonics, 2020, 7, 1699-1707.	3.2	112
38	Directional perfect absorption using deep subwavelength low-permittivity films. Physical Review B, 2014, 90, .	1.1	111
39	Micrometer‧cale Cubic Unit Cell 3D Metamaterial Layers. Advanced Materials, 2010, 22, 5053-5057.	11.1	109
40	Strong Coupling between Nanoscale Metamaterials and Phonons. Nano Letters, 2011, 11, 2104-2108.	4.5	109
41	Collection-mode near-field imaging with 0.5-THz pulses. IEEE Journal of Selected Topics in Quantum Electronics, 2001, 7, 600-607.	1.9	108
42	Nonpolar InGaN/GaN Core–Shell Single Nanowire Lasers. Nano Letters, 2017, 17, 1049-1055.	4.5	103
43	Terahertz emission from electric field singularities in biased semiconductors. Optics Letters, 1996, 21, 1924.	1.7	100
44	Coherent double-pulse control of quantum beats in a coupled quantum well. Physical Review B, 1993, 48, 11043-11050.	1.1	94
45	Metamaterials for THz polarimetric devices. Optics Express, 2009, 17, 773.	1.7	93
46	Multistage dispersion compensator using ring resonators. Optics Letters, 1999, 24, 1555.	1.7	90
47	Ill–V Semiconductor Nanoresonators—A New Strategy for Passive, Active, and Nonlinear Allâ€Dielectric Metamaterials. Advanced Optical Materials, 2016, 4, 1457-1462.	3.6	82
48	Multipolar Coupling in Hybrid Metal–Dielectric Metasurfaces. ACS Photonics, 2016, 3, 349-353.	3.2	79
49	Efficient wide-band and tunable midspan spectral inverter using cascaded nonlinearities in LiNbO3 waveguides. IEEE Photonics Technology Letters, 2000, 12, 82-84.	1.3	77
50	High-resolution zero-dispersion wavelength mapping in single-mode fiber. Optics Letters, 1998, 23, 1520.	1.7	75
51	Polarization-Dependent Second Harmonic Diffraction from Resonant GaAs Metasurfaces. ACS Photonics, 2018, 5, 1786-1793.	3.2	74
52	Carrier Dynamics and Electro-Optical Characterization of High-Performance GaN/InGaN Core-Shell Nanowire Light-Emitting Diodes. Scientific Reports, 2018, 8, 501.	1.6	69
53	Terahertz electromagnetic radiation from quantum wells. Applied Physics B: Lasers and Optics, 1994, 58, 249-259.	1.1	67
54	Growth of Ga-face and N-face GaN films using ZnO Substrates. MRS Internet Journal of Nitride Semiconductor Research, 1996, 1, 1.	1.0	67

#	Article	IF	CITATIONS
55	Nonresonant Broadband Funneling of Light via Ultrasubwavelength Channels. Physical Review Letters, 2011, 107, 163902.	2.9	66
56	Photoconductive Terahertz Near-Field Detector with a Hybrid Nanoantenna Array Cavity. ACS Photonics, 2015, 2, 1763-1768.	3.2	66
57	Pressure compression of CdSe nanoparticles into luminescent nanowires. Science Advances, 2017, 3, e1602916.	4.7	66
58	Huygens' Metasurfaces Enabled by Magnetic Dipole Resonance Tuning in Split Dielectric Nanoresonators. Nano Letters, 2017, 17, 4297-4303.	4.5	66
59	All-optical switching of an epsilon-near-zero plasmon resonance in indium tin oxide. Nature Communications, 2021, 12, 1017.	5.8	66
60	Nonlinear frequency conversion in optical nanoantennas and metasurfaces: materials evolution and fabrication. Opto-Electronic Advances, 2018, 1, 18002101-18002112.	6.4	65
61	Fabrication of 3D Metamaterial Resonators Using Selfâ€Aligned Membrane Projection Lithography. Advanced Materials, 2010, 22, 3171-3175.	11.1	64
62	Active tuning of mid-infrared metamaterials by electrical control of carrier densities. Optics Express, 2012, 20, 1903.	1.7	64
63	Multi-Colour Nanowire Photonic Crystal Laser Pixels. Scientific Reports, 2013, 3, 2982.	1.6	64
64	Near-Field Mapping of Optical Modes on All-Dielectric Silicon Nanodisks. ACS Photonics, 2014, 1, 794-798.	3.2	64
65	Single-mode lasing of GaN nanowire-pairs. Applied Physics Letters, 2012, 101, .	1.5	63
66	Terahertz Detection with Perfectly-Absorbing Photoconductive Metasurface. Nano Letters, 2019, 19, 2888-2896.	4.5	63
67	Metalorganic molecular beam epitaxy of InP, Ga0.47In0.53As, and GaAs with tertiarybutylarsine and tertiarybutylphosphine. Applied Physics Letters, 1990, 56, 1448-1450.	1.5	61
68	Second harmonic generation from metamaterials strongly coupled to intersubband transitions in quantum wells. Applied Physics Letters, 2014, 104, .	1.5	61
69	Coherent control of terahertz emission and carrier populations in semiconductor heterostructures. Journal of the Optical Society of America B: Optical Physics, 1994, 11, 2457.	0.9	59
70	Near-field microscope probe for far infrared time domain measurements. Applied Physics Letters, 2000, 77, 591-593.	1.5	57
71	Anisotropic optical properties of (110)-oriented quantum wells. Physical Review B, 1991, 44, 1930-1933.	1.1	56
72	3 <i>μ</i> m aperture probes for near-field terahertz transmission microscopy. Applied Physics Letters, 2014, 104, .	1.5	55

#	Article	IF	CITATIONS
73	Particle localization and phonon sidebands in GaAs/AlxGa1â^'xAs multiple quantum wells. Physical Review B, 1992, 46, 7927-7930.	1.1	50
74	Generation of terahertz electromagnetic pulses from quantum-well structures. IEEE Journal of Quantum Electronics, 1994, 30, 1478-1488.	1.0	49
75	Efficient photoconductive terahertz detector with all-dielectric optical metasurface. APL Photonics, 2018, 3, .	3.0	49
76	Design and nonlinear servo control of MEMS mirrors and their performance in a large port-count optical switch. Journal of Microelectromechanical Systems, 2005, 14, 261-273.	1.7	47
77	Epsilon-Near-Zero Modes for Tailored Light-Matter Interaction. Physical Review Applied, 2015, 4, .	1.5	46
78	ScAlMgO ₄ : an Oxide Substrate for GaN Epitaxy. MRS Internet Journal of Nitride Semiconductor Research, 1996, 1, 1.	1.0	45
79	A microfluidic system combining acoustic and dielectrophoretic particle preconcentration and focusing. Sensors and Actuators B: Chemical, 2008, 130, 645-652.	4.0	45
80	Frequency Conversion in a Time-Variant Dielectric Metasurface. Nano Letters, 2020, 20, 7052-7058.	4.5	45
81	Experimental evidence of Bragg confinement of carriers in a quantum barrier. Applied Physics Letters, 1992, 61, 949-951.	1.5	44
82	Active tuning of high-Q dielectric metasurfaces. Applied Physics Letters, 2017, 111, .	1.5	44
83	Shallow quantum well excitons: 2D or 3D?. Physical Review Letters, 1993, 70, 319-322.	2.9	43
84	Polarisation-insensitive wavelength converter based on cascaded nonlinearities in LiNbO3 waveguides. Electronics Letters, 2000, 36, 66.	0.5	43
85	Large-area metamaterials on thin membranes for multilayer and curved applications at terahertz and higher frequencies. Applied Physics Letters, 2009, 94, 161113.	1.5	42
86	Tunable metamaterials based on voltage controlled strong coupling. Applied Physics Letters, 2013, 103, 263116.	1.5	40
87	Gain spectra and stimulated emission in epitaxial (In,Al) GaN thin films. Applied Physics Letters, 1996, 69, 3384-3386.	1.5	39
88	Doping tunable resonance: Toward electrically tunable mid-infrared metamaterials. Applied Physics Letters, 2010, 96, .	1.5	38
89	Nano-lithographically fabricated titanium dioxide based visible frequency three dimensional gap photonic crystal. Optics Express, 2007, 15, 13049.	1.7	37
90	Repetitive excitation of charge oscillations in semiconductor heterostructures. Applied Physics Letters, 1993, 63, 2213-2215.	1.5	36

#	Article	IF	CITATIONS
91	Distributed feedback gallium nitride nanowire lasers. Applied Physics Letters, 2014, 104, .	1.5	36
92	Transient GaAs Plasmonic Metasurfaces at Terahertz Frequencies. ACS Photonics, 2017, 4, 15-21.	3.2	36
93	All-optical tuning of symmetry protected quasi bound states in the continuum. Applied Physics Letters, 2019, 115, .	1.5	36
94	Towards an Integrated Microneedle Total Analysis Chip for Protein Detection. Electroanalysis, 2016, 28, 1305-1310.	1.5	35
95	Polarimetry Using Graphene-Integrated Anisotropic Metasurfaces. ACS Photonics, 2018, 5, 4283-4288.	3.2	35
96	Third-harmonic generation from Mie-type resonances of isolated all-dielectric nanoparticles. Philosophical Transactions Series A, Mathematical, Physical, and Engineering Sciences, 2017, 375, 20160281.	1.6	34
97	Near-field probing of Mie resonances in single TiO_2 microspheres at terahertz frequencies. Optics Express, 2014, 22, 23034.	1.7	33
98	Quantum-Size-Controlled Photoelectrochemical Fabrication of Epitaxial InGaN Quantum Dots. Nano Letters, 2014, 14, 5616-5620.	4.5	33
99	Perfectly absorbing dielectric metasurfaces for photodetection. APL Photonics, 2020, 5, .	3.0	33
100	160 Gbit/s wavelength shifting and phase conjugation using periodically poled LiNbO3 waveguide parametric converter. Electronics Letters, 2000, 36, 1788.	0.5	32
101	Electrostatic Actuation of Three-Dimensional MEMS Mirrors Using Sidewall Electrodes. IEEE Journal of Selected Topics in Quantum Electronics, 2004, 10, 472-477.	1.9	32
102	Gold substrate-induced single-mode lasing of GaN nanowires. Applied Physics Letters, 2012, 101, 221114.	1.5	32
103	Efficient infrared thermal emitters based on low-albedo polaritonic meta-surfaces. Applied Physics Letters, 2013, 102, .	1.5	32
104	Intrinsic polarization control in rectangular GaN nanowire lasers. Nanoscale, 2016, 8, 5682-5687.	2.8	32
105	Nanocomposite plasmonic fluorescence emitters with core/shell configurations. Journal of the Optical Society of America B: Optical Physics, 2010, 27, 1561.	0.9	31
106	Interaction between metamaterial resonators and intersubband transitions in semiconductor quantum wells. Applied Physics Letters, 2011, 98, 203103.	1.5	31
107	Doping-tunable thermal emission from plasmon polaritons in semiconductor epsilon-near-zero thin films. Applied Physics Letters, 2014, 105, .	1.5	31
108	Tunable all-optical time-slot-interchange and wavelength conversion using difference-frequency-generation and optical buffers. IEEE Photonics Technology Letters, 2002, 14, 200-202.	1.3	30

#	Article	IF	CITATIONS
109	Near-Field Spectroscopy and Imaging of Subwavelength Plasmonic Terahertz Resonators. IEEE Transactions on Terahertz Science and Technology, 2016, 6, 382-388.	2.0	30
110	Tailoring the morphology and luminescence of GaN/InGaN core–shell nanowires using bottom-up selective-area epitaxy. Nanotechnology, 2017, 28, 025202.	1.3	30
111	Modular MEMS-based optical cross-connect with large port-count. IEEE Photonics Technology Letters, 2003, 15, 1773-1775.	1.3	29
112	Internal quantum efficiency and carrier dynamics in semipolar (20		

	Letters, 2015, 15, 1959-1966.		
114	Theory and modeling of electrically tunable metamaterial devices using inter-subband transitions in semiconductor quantum wells. Optics Express, 2012, 20, 6584.	1.7	27
115	Virtual excitation of the Fermi-edge singularity in modulation-doped quantum wells. Physical Review B, 1995, 51, 2005-2008.	1.1	26
116	Electrically tunable infrared metamaterials based on depletion-type semiconductor devices. Journal of Optics (United Kingdom), 2012, 14, 114013.	1.0	26
117	Simultaneous Detection of Dopamine, Ascorbic Acid and Uric Acid at Lithographicallyâ€Defined 3D Graphene Electrodes. Electroanalysis, 2014, 26, 52-56.	1.5	26
118	Broadband and Efficient Second-Harmonic Generation from a Hybrid Dielectric Metasurface/Semiconductor Quantum-Well Structure. ACS Photonics, 2019, 6, 1458-1465.	3.2	26
119	Ultrafast optical switching and power limiting in intersubband polaritonic metasurfaces. Optica, 2021, 8, 606.	4.8	26
120	THz radiation from coherent population changes in quantum wells. Physical Review B, 1994, 49, 4668-4672.	1.1	25
121	Effect of thin silicon dioxide layers on resonant frequency in infrared metamaterials. Optics Express, 2010, 18, 1085.	1.7	25
122	Optical Strong Coupling between near-Infrared Metamaterials and Intersubband Transitions in III-Nitride Heterostructures. ACS Photonics, 2014, 1, 906-911.	3.2	25
123	Enhanced optical nonlinearities in the near-infrared using III-nitride heterostructures coupled to metamaterials. Applied Physics Letters, 2015, 107, .	1.5	25
124	Controlled Growth of Ordered III-Nitride Core–Shell Nanostructure Arrays for Visible Optoelectronic Devices. Journal of Electronic Materials, 2015, 44, 1255-1262.	1.0	25
125	Low-Power Absorption Saturation in Semiconductor Metasurfaces. ACS Photonics, 2019, 6, 2797-2806.	3.2	25
126	Terahertz near-field imaging. Physics in Medicine and Biology, 2002, 47, 3727-3734.	1.6	24

#	Article	IF	CITATIONS
127	Near-infrared surface plasmon polariton dispersion control with hyperbolic metamaterials. Optics Express, 2013, 21, 11107.	1.7	24
128	Electrodynamic modeling of strong coupling between a metasurface and intersubband transitions in quantum wells. Physical Review B, 2014, 89, .	1.1	24
129	An All-Dielectric Polaritonic Metasurface with a Giant Nonlinear Optical Response. Nano Letters, 2022, 22, 896-903.	4.5	22
130	Stability and bandwidth enhancement of difference frequency generation (DFG)-based wavelength conversion by pump detuning. Electronics Letters, 1999, 35, 978.	0.5	21
131	The Role of Liquid Ink Transport in the Direct Placement of Quantum Dot Emitters onto Subâ€Micrometer Antennas by Dipâ€Pen Nanolithography. Small, 2018, 14, e1801503.	5.2	21
132	Nonlinear optical study of the Fermi edge singularity: differences from atomic excitons in the virtual excitation regime. Journal of the Optical Society of America B: Optical Physics, 1996, 13, 1313.	0.9	20
133	Probing terahertz surface plasmon waves in graphene structures. Applied Physics Letters, 2013, 103, .	1.5	20
134	Continuous and dynamic spectral tuning of single nanowire lasers with subnanometer resolution using hydrostatic pressure. Nanoscale, 2015, 7, 9581-9588.	2.8	20
135	Refractive index sensing with Fano resonances in silicon oligomers. Philosophical Transactions Series A, Mathematical, Physical, and Engineering Sciences, 2017, 375, 20160070.	1.6	20
136	Terahertz Pulse Generation from GaAs Metasurfaces. ACS Photonics, 2022, 9, 1136-1142.	3.2	20
137	Realization of tellurium-based all dielectric optical metamaterials using a multi-cycle deposition-etch process. Applied Physics Letters, 2013, 102, 161905.	1.5	19
138	Chemoselective gas sensors based on plasmonic nanohole arrays. Optical Materials Express, 2012, 2, 1655.	1.6	18
139	Annular-Shaped Emission from Gallium Nitride Nanotube Lasers. ACS Photonics, 2015, 2, 1025-1029.	3.2	18
140	Strong Coupling in All-Dielectric Intersubband Polaritonic Metasurfaces. Nano Letters, 2021, 21, 367-374.	4.5	18
141	Cascaded (2) wavelength converter in LiNbO3 waveguides with counter-propagating beams. Electronics Letters, 1999, 35, 1155.	0.5	17
142	High-Q terahertz Fano resonance with extraordinary transmission in concentric ring apertures. Optics Express, 2014, 22, 3747.	1.7	17
143	Annealing of Cdâ€implanted GaAs: Defect removal, lattice site occupation, and electrical activation. Journal of Applied Physics, 1993, 73, 4248-4256.	1.1	16
144	External modulators for TeraHertz Quantum Cascade Lasers based on electrically-driven active metamaterials. Metamaterials, 2010, 4, 83-88.	2.2	16

#	Article	IF	CITATIONS
145	Phase resolved near-field mode imaging for the design of frequency-selective surfaces. Optics Express, 2012, 20, 11986.	1.7	16
146	Quantum-Dot-Based Solid-State Lighting With Electric-Field-Tunable Chromaticity. Journal of Display Technology, 2013, 9, 419-426.	1.3	16
147	Label-Free Plasmonic Immunosensing for Plasmodium in a Whole Blood Lysate. IEEE Sensors Journal, 2014, 14, 1399-1404.	2.4	16
148	Fabrication of Hollow Metal Microneedle Arrays Using a Molding and Electroplating Method. MRS Advances, 2019, 4, 1417-1426.	0.5	16
149	Splitting of magnetic dipole modes in anisotropic TiO ₂ microâ€spheres. Laser and Photonics Reviews, 2016, 10, 681-687.	4.4	15
150	Solitary Oxygen Dopant Emission from Carbon Nanotubes Modified by Dielectric Metasurfaces. ACS Nano, 2017, 11, 6431-6439.	7.3	15
151	Polarization control in GaN nanowire lasers. Optics Express, 2014, 22, 19198.	1.7	14
152	Detection of internal fields in double-metal terahertz resonators. Applied Physics Letters, 2017, 110, .	1.5	14
153	Ultrafast all-optical diffraction switching using semiconductor metasurfaces. Applied Physics Letters, 2021, 118, .	1.5	14
154	Manipulation of Exciton Dynamics in Single-Layer WSe ₂ Using a Toroidal Dielectric Metasurface. Nano Letters, 2021, 21, 9930-9938.	4.5	14
155	Reduction of Cross-Phase Modulation-Induced Impairments in Long-Haul WDM Telecommunication Systems Via Spectral Inversion. IEEE Photonics Technology Letters, 2004, 16, 677-679.	1.3	13
156	Polarization-dependent photocurrent enhancement in metamaterial-coupled quantum dots-in-a-well infrared detectors. Optics Communications, 2014, 312, 31-34.	1.0	13
157	Characterization of an active metasurface using terahertz ellipsometry. Applied Physics Letters, 2017, 111, .	1.5	13
158	Terahertz Driven Amplification of Coherent Optical Phonons in GaAs Coupled to a Metasurface. Physical Review Letters, 2019, 122, 107402.	2.9	13
159	Energy Frontier Research Center for Solid-State Lighting Science: Exploring New Materials Architectures and Light Emission Phenomena. Journal of Physical Chemistry C, 2014, 118, 13330-13345.	1.5	12
160	Differenceâ€Frequency Generation in Polaritonic Intersubband Nonlinear Metasurfaces. Advanced Optical Materials, 2018, 6, 1800681.	3.6	12
161	Mid-infrared second-harmonic generation in ultra-thin plasmonic metasurfaces without a full-metal backplane. Applied Physics B: Lasers and Optics, 2018, 124, 1.	1.1	12
162	Observation of Intersubband Polaritons in a Single Nanoantenna Using Nano-FTIR Spectroscopy. Nano Letters, 2019, 19, 4620-4626.	4.5	12

#	Article	IF	CITATIONS
163	Highly efficient terahertz photoconductive metasurface detectors operating at microwatt-level gate powers. Optics Letters, 2021, 46, 3159.	1.7	12
164	Cascaded Optical Nonlinearities in Dielectric Metasurfaces. ACS Photonics, 2022, 9, 1026-1032.	3.2	12
165	Mid-infrared time-domain spectroscopy system with carrier-envelope phase stabilization. Applied Physics Letters, 2013, 103, 181111.	1.5	11
166	Decay times of excitons in latticeâ€matched InGaAs/InP single quantum wells. Applied Physics Letters, 1991, 58, 965-967.	1.5	10
167	A metasurface optical modulator using voltage-controlled population of quantum well states. Applied Physics Letters, 2018, 113, 201101.	1.5	10
168	Localized and extended exciton states in narrow GaAs/AlGaAs quantum wells. Superlattices and Microstructures, 1989, 5, 223-226.	1.4	9
169	Spectral filtering using active metasurfaces compatible with narrow bandgap III-V infrared detectors. Optics Express, 2016, 24, 21512.	1.7	9
170	Low dissipation spectral filtering using a field-effect tunable III–V hybrid metasurface. Applied Physics Letters, 2018, 113, .	1.5	9
171	Noninvasive Nearâ€Field Spectroscopy of Single Subwavelength Complementary Resonators. Laser and Photonics Reviews, 2020, 14, 1900254.	4.4	9
172	Coherent Terahertz Radiation from Cavity Polaritons in GaAs/AlGaAs Microcavities. Physica Status Solidi A, 2000, 178, 365-372.	1.7	8
173	Defect-assisted plasmonic crystal sensor. Optics Letters, 2013, 38, 2569.	1.7	8
174	Multipolar second harmonic generation in a symmetric nonlinear metamaterial. Scientific Reports, 2017, 7, 8101.	1.6	8
175	Interchannel cross talk caused by pump depletion in periodically poled LiNbO_3 waveguide wavelength converters. Journal of the Optical Society of America B: Optical Physics, 2002, 19, 849.	0.9	7
176	Diagnostic Devices: Microneedleâ€Based Transdermal Sensor for Onâ€Chip Potentiometric Determination of K ⁺ (Adv. Healthcare Mater. 6/2014). Advanced Healthcare Materials, 2014, 3, 948-948.	3.9	7
177	Part-Per-Trillion Level Detection of Microcystin-LR Using a Periodic Nanostructure. IEEE Sensors Journal, 2015, 15, 1366-1371.	2.4	7
178	Resonant Raman scattering mediated by intrinsic excitons inCd1â^'xZnxTe (xâ^1⁄40.5). Physical Review B, 1989, 40, 8313-8318.	1.1	6
179	Resonant Raman scattering by acceptors in GaAs/AlxGa1â^'xAs multiple quantum wells: A probe of exciton localization. Physical Review B, 1990, 42, 11035-11041.	1.1	6
180	Enhancing Absorption Bandwidth through Vertically Oriented Metamaterials. Applied Sciences (Switzerland), 2019, 9, 2223.	1.3	6

#	Article	IF	CITATIONS
181	Manipulation of quantum dot emission with semiconductor metasurfaces exhibiting magnetic quadrupole resonances. Optics Express, 2021, 29, 5567.	1.7	6
182	Nonuniform Morphology and Luminescence Properties of a Molecular Beam Epitaxy GaN Film from Atomic Force Microscopy, Scanning Electron Microscopy and Cathodoluminescence. MRS Internet Journal of Nitride Semiconductor Research, 1997, 2, 1.	1.0	5
183	Fabrication techniques for three-dimensional metamaterials in the midinfrared. Journal of Vacuum Science and Technology B:Nanotechnology and Microelectronics, 2010, 28, C6O30-C6O33.	0.6	5
184	Label-free plasmonic immunosensing for plasmodium in whole blood. , 2013, , .		5
185	Electrodeposited Iron as a Biocompatible Material for Microneedle Fabrication. Electroanalysis, 2015, 27, 2239-2249.	1.5	5
186	Spectrally-resolved internal quantum efficiency and carrier dynamics of semipolar \$(10ar{1}1)\$ core-shell triangular nanostripe GaN/InGaN LEDs. Nanotechnology, 2018, 29, 235206.	1.3	5
187	Dynamic membrane projection lithography [Invited]. Optical Materials Express, 2011, 1, 962.	1.6	4
188	Releasable infrared metamaterials. Journal of Vacuum Science and Technology B:Nanotechnology and Microelectronics, 2011, 29, 051806.	0.6	4
189	Quenching of Infrared-Active Optical Phonons in Nanolayers of Crystalline Materials by Graphene Surface Plasmons. ACS Photonics, 2018, 5, 2706-2711.	3.2	4
190	All-dielectric photoconductive metasurfaces for terahertz applications. Photoniques, 2020, , 47-52.	0.0	4
191	Resonant raman scattering by acceptors and LO phonons in GaAs/AlGaAs multiple quantum wells. Surface Science, 1990, 228, 180-183.	0.8	3
192	CdSe infiltrated TiO2 based omnidirectional photonic crystals for visible light control. Photonics and Nanostructures - Fundamentals and Applications, 2008, 6, 12-18.	1.0	3
193	Metamaterials: Micrometer-Scale Cubic Unit Cell 3D Metamaterial Layers (Adv. Mater. 44/2010). Advanced Materials, 2010, 22, 4916-4916.	11.1	3
194	Dark-State-Based Low-Loss Metasurfaces with Simultaneous Electric and Magnetic Resonant Response. ACS Photonics, 2020, 7, 241-248.	3.2	3
195	Structural tuning of nonlinear terahertz metamaterials using broadside coupled split ring resonators. AIP Advances, 2021, 11, .	0.6	3
196	Nanostructured photoconductive terahertz detector for near-field microscopy. , 2016, , .		2
197	Nonlinear and ultrafast effects. , 2020, , 223-248.		2
198	Dielectric metasurfaces made from vertically oriented nanoresonators. Journal of the Optical Society of America B: Optical Physics, 2021, 38, C33.	0.9	2

#	Article	IF	CITATIONS
199	Ultrafast all-optical tuning of magnetic modes in GaAs metasurfaces. , 2017, , .		2
200	Terahertz detectors based on all-dielectric photoconductive metasurfaces. , 2019, , .		2
201	Ultrafast optical switching and power limiting in intersubband polaritonic metasurfaces. , 2020, , .		2
202	Nonlinear and Ultrafast All-Dielectric Metasurfaces at the Center for Integrated Nanotechnologies. Nanotechnology, 0, , .	1.3	2
203	Intervalence-band photoinduced absorption in undoped GaAs/AlxGa1â^'xAs multiple-quantum-wells. Superlattices and Microstructures, 1990, 7, 291-293.	1.4	1
204	Introduction to the Topical Issue on Laser Dynamics and Nonlinear Photonics. European Physical Journal D, 2010, 58, 153-159.	0.6	1
205	Resonant coupling to a dipole absorber inside a metamaterial: Anticrossing of the negative index response. Journal of Vacuum Science and Technology B:Nanotechnology and Microelectronics, 2010, 28, C6O16-C6O20.	0.6	1
206	Metamaterial based devices for terahertz imaging. , 2010, , .		1
207	Multilayer infrared metamaterial fabrication using membrane projection lithography. Journal of Vacuum Science and Technology B:Nanotechnology and Microelectronics, 2011, 29, 06FF04.	0.6	1
208	Optical Manipulation with Plasmonic Beam Shaping Antenna Structures. Advances in OptoElectronics, 2012, 2012, 1-6.	0.6	1
209	Defect-assisted plasmonic sensing. , 2013, , .		1
210	Gallium Nitride Nanotube Lasers. , 2014, , .		1
211	Liquid Crystal Tuning of All-dielectric Metasurfaces. , 2015, , .		1
212	Dielectric Resonators: III–V Semiconductor Nanoresonators—A New Strategy for Passive, Active, and Nonlinear Allâ€Dielectric Metamaterials (Advanced Optical Materials 10/2016). Advanced Optical Materials, 2016, 4, 1658-1658.	3.6	1
213	Near-field THz time-domain spectroscopy of anisotropic dielectric micro-particles. , 2016, , .		1
214	Splitting of magnetic dipole modes in anisotropic TiO2micro-spheres (Laser Photonics Rev. 10(4)/2016). Laser and Photonics Reviews, 2016, 10, 698-698.	4.4	1
215	Parametric Analysis of Vertically Oriented Metamaterials for Wideband Omnidirectional Perfect Absorption. , 2018, , .		1
216	Intensity-dependent reflectance modulation of femtosecond laser pulses in GaAs nanocylinders with magnetic resonances. Journal of Physics: Conference Series, 2018, 1092, 012181.	0.3	1

#	Article	IF	CITATIONS
217	Control of Second-Harmonic Generation in Dielectric Polaritonic Metasurfaces Using χ(2) Polarity Switching. , 2021, , .		1
218	3D metamaterials for thermal-IR applications. SPIE Newsroom, 0, , .	0.1	1
219	Demonstration of Dielectric Optical Magnetic Mirrors Using Phase-locked Infrared Time-domain Spectroscopy. , 2013, , .		1
220	All-Dielectric Intersubband Polaritonic Metasurface with Giant Second-Order Nonlinear Response. , 2020, , .		1
221	Tailoring Second Harmonic Diffraction in GaAs Metasurfaces via Crystal Orientation. , 2019, , .		1
222	Electrically Tunable Mid-Infrared Metamaterials Based on Strong Light-Matter Coupling. , 2014, , .		1
223	Active Tuning of High-Q Dielectric Metasurfaces by Liquid Crystals. , 2018, , .		1
224	An efficient terahertz detector based on an optical hybrid cavity. , 2018, , .		1
225	All-Optical Tuning of Fano Resonances in Broken Symmetry GaAs Metasurfaces. , 2019, , .		1
226	Tunable Fully Absorbing Metasurfaces for Efficient THz Detection. , 2020, , .		1
227	Resonant Raman scattering mediated by excitons in CdTe/CdZnTe multiple quantum wells. Journal of Luminescence, 1992, 53, 348-350.	1.5	0
228	Direct observation of optical magnetism from a dielectric resonator metamaterial using time-domain spectroscopy in the mid-infrared. , 2012, , .		0
229	New Directions in Active and Tunable Metamaterials. , 2013, , .		0
230	Gallium Nitride Nanowire Distributed Feedback Lasers. , 2014, , .		0
231	Shaping Emission Spectra of Quantum Dots by All-dielectric Metasurfaces. , 2014, , .		Ο
232	Metamaterials strongly coupled to intersubband transitions: Circuit model and second order nonlinear processes. , 2014, , .		0
233	Second harmonic generation in quantum wells enhanced via coupling to metamaterials. , 2014, , .		0
234	Maximizing Strong Coupling between Metasurface Resonators and Intersubband Transitions. , 2014, , .		0

#	Article	IF	CITATIONS
235	Magnetic dipole and electric dipole resonances in TiO2microspheres at terahertz frequencies. , 2015, , .		Ο
236	Third-Harmonic Generation from Silicon Oligomers and Metasurfaces. , 2015, , .		0
237	What is an epsilon-near-zero mode?. , 2015, , .		0
238	Terahertz near-field spectroscopy through a sub-wavelength size aperture. , 2015, , .		0
239	Plasmonic enhancement of sensitivity in terahertz (THz) photo-conductive detectors. , 2015, , .		0
240	Third harmonic generation in isolated all dielectric meta-atoms (Conference Presentation). , 2016, , .		0
241	Tailoring dielectric resonator geometries for directional scattering, Huygens' metasurfaces, and high quality-factor Fano resonances. , 2016, , .		0
242	III-Nitride nanowires lasers. , 2016, , .		0
243	Plasmonic resonances in carbon fibers observed with terahertz near-field microscopy. Proceedings of SPIE, 2016, , .	0.8	0
244	Spectroscopy and mapping of resonant fields in terahertz plasmonic resonators. , 2017, , .		0
245	Flat nonlinear optics: metasurfaces for efficient frequency mixing. , 2017, , .		0
246	Ultrafast modulation of femtosecond laser pulses in direct-gap semiconductor metasurfaces with magnetic resonances. AlP Conference Proceedings, 2017, , .	0.3	0
247	Top-down fabrication for III-nitride nanophotonics. , 2017, , .		Ο
248	Designing an efficient hybrid optical cavity. , 2017, , .		0
249	A Hybrid Dielectric-Semiconductor Metasurface for Efficient Second-Harmonic Generation. , 2018, , .		0
250	Optical Nonlinearities in All-Dielectric Metasurfaces. , 2018, , .		0
251	Precision Additive Nanofabrication: The Role of Liquid Ink Transport in the Direct Placement of Quantum Dot Emitters onto Sub-Micrometer Antennas by Dip-Pen Nanolithography (Small 31/2018). Small, 2018, 14, 1870144.	5.2	0
252	Efficient Terahertz Detection with Perfectly-Absorbing Metasurface. , 2019, , .		0

#	Article	IF	CITATIONS
253	Probe-Sample Interaction in Aperture-type THz Near-Field Microscopy of Complementary Resonators. , 2019, , .		0
254	Hybrid Dielectric Metasurfaces: From Strong Light-Matter Interaction to Extreme Nonlinearities. , 2019, , .		0
255	All-Dielectric Metasurfaces: Optical Nonlinearities and Emission Control. , 2019, , .		0
256	Dielectric Metasurfaces made of Vertically Oriented Germanium Ellipses. , 2021, , .		0
257	Ultrafast and Nonlinear Semiconductor Metasurfaces. , 2021, , .		0
258	Ultrafast and Nonlinear Semiconductor Metasurfaces. , 2021, , .		0
259	Merging Magnetic and Electric Resonances for All-Dielectric Nanoantenna Arrays. , 2013, , .		0
260	Realization of Tellurium-based all Dielectric Optical Metamaterials using a Multi-cycle Deposition-etch Process. , 2013, , .		0
261	Apertureless Optical Near-Field Imaging of Localized Modes of Silicon Nanodisks. , 2014, , .		0
262	Optical Generation of Terahertz Pulses in Quantum Wells. , 1993, , .		0
263	Coherent Second Harmonic Generation in a Quantum Well-Metasurface Coupled System. , 2015, , .		0
264	Wide and reversible tuning of an individual nanowire laser using hydrostatic pressure. , 2015, , .		0
265	Tailored Light-Matter Interaction through Epsilon-Near-Zero Modes. , 2015, , .		0
266	Highly-Efficient Polarization-Insensitive Holograms Based on Dielectric Metasurfaces. , 2016, , .		0
267	Ultrafast Dynamics of Epsilon-Near-Zero Modes in GaAs at Terahertz Frequencies. , 2016, , .		0
268	2D and 3D all dielectric metamaterials made from III-V semiconductors. , 2016, , .		0
269	Intrinsic Properties of Anisotropic Dielectric Micro-Resonators Obtained through Near-Field Terahertz Spectroscopy. , 2016, , .		0
270	Efficient second harmonic generation from GaAs all-dielectric metasurfaces. , 2016, , .		0

#	Article	IF	CITATIONS
271	III-V dielectric metasurfaces: enhanced nonlinearities and emission control. , 2017, , .		0
272	Nonlinear Metamaterials: Breaking the Dipole Approximation. , 2017, , .		0
273	High-Contrast, All-Optical Switching of Infrared Light using a Cadmium Oxide Perfect Absorber. , 2017, , .		Ο
274	Enhanced Sensitivity of Terahertz Allergen Sensors Based on Complementary Metasurfaces. , 2017, , .		0
275	Extreme Nonlinear Optics with Dielectric Metasurfaces. , 2019, , .		0
276	A Hybrid Dielectric-Semiconductor Resonant Nanostructure for Broadband and Efficient Second-Harmonic Generation. , 2019, , .		0
277	Zirconium metal-organic framework functionalized plasmonic sensor. , 2019, , .		0
278	Frequency Conversion in a Dielectric Time-Variant Metasurface via Optical Pumping. , 2020, , .		0
279	Intersubband Polaritons and Strong Coupling in Single Nanoantenna Observed by Near-field Microscopy. , 2020, , .		0
280	Photoconductive Metasurfaces for Terahertz Detection. , 2020, , .		0
281	Cascaded Third Harmonic Generation in Dielectric Metasurfaces. , 2020, , .		0
282	Light-matter Interaction and Third Harmonic Generation in the Near-infrared Using Plasmonic Metasurfaces and InAs/AISb Semiconductor Heterostructures. , 2020, , .		0
283	Ultrafast Diffraction Switching Using GaAs Metasurfaces. , 2020, , .		Ο
284	Intersubband Polaritonics in Dielectric Metasurfaces. , 2020, , .		0
285	Correction to "Terahertz Pulse Generation from GaAs Metasurfaces― ACS Photonics, 0, , .	3.2	Ο